Investigation of Carbon Fiber Reinforced Plastics Machining Using 355 nm Picosecond Pulsed Laser

Jun Hu[1] · Dezhi Zhu[2]

Abstract Carbon fiber reinforced plastics (CFRP) has been widely used in the aircraft industry and automobile industry owing to its superior properties. In this paper, a Nd:YVO4 picosecond pulsed system emitting at 355 nm has been used for CFRP machining experiments to determine optimum milling conditions. Milling parameters including laser power, milling speed and hatch distance were optimized by using box-behnken design of response surface methodology (RSM). Material removal rate was influenced by laser beam overlap ratio which affects mechanical denudation. The results in heat affected zones (HAZ) and milling quality were discussed through the machined surface observed with scanning electron microscope. A re-focusing technique based on the experiment with different focal planes was proposed and milling mechanism was also analyzed in details.

1 Introduction

Carbon fiber reinforced plastics (CFRP) gains significant importance in the aircraft and automobile industries owing to its durable benefits and superior ratio of strength to weight. Therefore, compared to metals, CFRP is increasingly being used in many weight-critical components. For instance, in Airbus A350, the composite content is over 30%, which reaches 50% when it comes to B787, a new aircraft of Boeing [1]. CFRP also plays an important role in other fields including environment and medicine.

CFRP consists of carbon fibers and resin matrix, which are different in characteristics. Carbon fiber has one order of magnitude higher evaporation temperature than resin matrix [2]. Because of CFRP's anisotropic and nonhomogeneous properties, it's difficult for mechanical machining and

✉ Jun Hu
  hjmorning@hotmail.com

1   College of Mechanical Engineering, Donghua University, Shanghai 201620, China

2   School of Mechanical Engineering, Shanghai Jiao Tong University, Shanghai 200240, China

laser milling of CFRP [3]. In mechanical machining including milling, grinding and sawing [4, 5], different properties result in serious tool wear, delamination and fiber pull-out [6].Therefore, researchers have proposed some non-traditional machining methods for CFRP processing such as water jet cutting [7], which needs specialized equipment and also causes delamination and poor mechanical properties because of moisture penetration into the material. Laser, as a non-contact and dry tool for material processing, has some unique advantages including ease of control, no machining force and no tool wear [8]. However, laser milling of CFRP also presents disadvantages, of which the most serious one is heat affected zone (HAZ). Yung K C et al. studied the influence of laser repetition frequencies and power on the HAZ [9].Traditional materials are isotropic, but the carbon fiber orientation is different in resin matrix. During laser milling, because of heat accumulation, the temperature rises, which results in decomposition of resin matrix before the vaporization temperature of carbon fibers is reached. This further causes matrix burnout [10]. Thus, it's necessary to suppress HAZ by reducing the laser-material interaction time. Short laser-material interaction time is a characteristic of picosecond lasers which enable low ablation thresholds [11].The unique properties of picosecond lasers have created new methods in materials processing with high peak intensities and high pulse repetition frequencies [12]. Thus, picosecond lasers are used widely in several applications.

In this paper, the investigation of CFRP laser milling was reported by using 355 nm picosecond pulsed laser ablation with 30 W diode pumped UV laser. Milling parameters including laser power, milling speed and hatch distance were optimized by using response surface methodology (RSM). According to the machined surface observed with scanning electron microscope, HAZ and milling quality were discussed and analyzed through milling mechanism. A re-focusing technique based on the experiment with different focal plane was proposed, which can be used to improve the material removal rate and suppress HAZ.

2 Experimental

2.1 CFRP Material

The CFRP material studied in this paper consists of seven laminates, with a thickness of 1.5 mm. Figure 1 shows the cross section of this CFRP which is composed of carbon fiber and matrix. The carbon fiber is T300, while the matrix is epoxy resin. The two external laminates are twill weave plies and other laminates are unidirectional 0° or unidirectional 90° with about 0.18 mm thickness. CFRP material properties are given in Table 1.
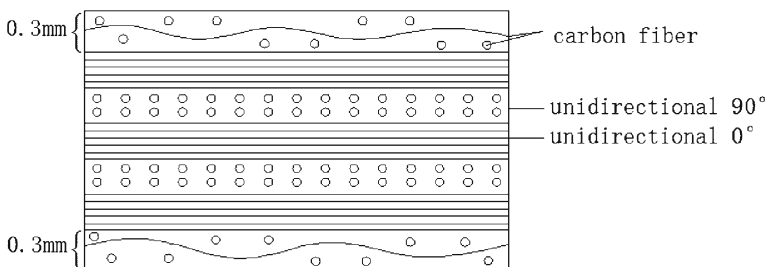

Fig. 1 Structure of the CFRP material

Table 1 Properties of the CFRP material

Property	Fiber	Matrix
Type	Carbon	Epoxy resin
Volume fraction	0.6	0.4
Vaporization temperature(°C)	3900	698
Density(kg/m^3)	1850	1200
Specific heat capacity(J/kg°C)	710	1884
Latent heat(kJ/kg)	43,000	1000

2.2 Laser Milling System

The laser source used in this experiment was 355 nm picosecond pulsed laser with 30 W diode pumped UV laser, and the pulse repetition rate is 400 kHz. The laser's pulse width is 10 ps. The maximum laser output power is 24 W. Figure 2 gives the draft of laser milling system which is composed of a UV laser source, b Optical signal, c scanner head, d F-theta lens, and e xyz motion platform. The laser beam with Guassian shape was focused on the surface of CFRP by the scanner head with the F-theta lens. The specimen was mounted on the xyz motion platform through which the focal plane whose spot size is 21 μm can be located on original surface. As shown in Fig. 2, the specimen was milled by the scanning pattern. The distance between the adjacent tracks is hatch distance.

2.3 Experimental Setup

The influence of process parameters including laser power (p), milling speed (v) and hatch distance (d) on surface quality and HAZ in UV laser milling was investigated and presented. Through the single factor experiments, the appropriate range of parameters are selected. The laser power was adjustable from 7.28w to 16.24w, milling speed varied between 2200 mm/s
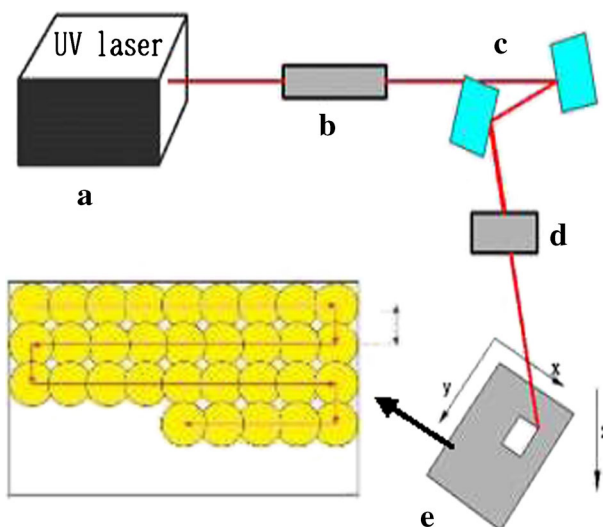
Fig. 2 Draft of laser milling system

and 2600 mm/s, and hatch distance was changed from 0.015 mm to 0.035 mm. The milling parameters were optimized through box-behnken design (BBD) of response surface methodology (RSM).

The machined surface of three specimens including the deepest one, the shallow one and the biggest HAZ were observed with scanning electron microscope.

A re-focusing technique experiment with different focal plane was proposed with three different z axis strategies varying five kinds of scanning passes, and the depths were measured with the three dimensional profilometer.

3 Results

In our previous research [13], the theoretical value of single pulse ablation depth without heat loss is

$$H = \frac{P/F}{f_c \pi r^2 \rho_c [C_c(T_c - T_a) + L_c] + f_e \pi r^2 \rho_e [C_e(T_e - T_a) + L_e]} \tag{1}$$

Where p is the laser power; F is the pulse repetition rate; r is the radius of focal spot; T_a is the operating ambient temperature; f_c, T_c, ρ_c, C_c, L_c are the volume fraction, vaporization temperature, density, Specific heat capacity, and latent heat of carbon fiber(c) and other parameters are the properties of epoxy resin(e).

There are some overlap section between pulses, and laser beam overlap ratio is

$$\alpha = \frac{\pi r^2 F}{vd} \tag{2}$$

Because of mechanical effects, the mechanical denudation factor is

$$\beta = \frac{h_a}{\alpha H} \tag{3}$$

Where h_a is the actual ablation depth milled at one pass, and after n passes the total actual ablation depth is h.

When CFRP material was milled by laser, the laser energy can be calculated as

$$E_L = \frac{npb}{v}\left(\frac{b-2r}{d} + 1\right) \tag{4}$$

Where b is the length of side of machined area. Through this research, the material removal rate (γ) can be denoted as

$$\gamma = \frac{hb^2}{E_L} = \frac{hbv}{np\left(\frac{b-2r}{d} + 1\right)} \tag{5}$$

3.1 Optimization of Milling Parameters

In order to evaluate the influence of process parameters on laser milling, milling depths, material removal rate and surface quality were analyzed. The average milling depths, average

Table 2 Experimental results

Trial	Power(w)	Milling speed(mm/s)	Hatch distance(mm)	Depth(μm)	β	γ(mm³/kJ)
1	7.28	2200	0.025	67	2.61	50.62
2	16.24	2200	0.025	105	1.84	35.56
3	7.28	2600	0.025	45	2.07	40.18
4	16.24	2600	0.025	84	1.74	33.62
5	7.28	2400	0.015	61	1.56	30.16
6	16.24	2400	0.015	124	1.42	27.49
7	7.28	2400	0.035	20	1.19	23.08
8	16.24	2400	0.035	69	1.84	35.69
9	11.76	2200	0.015	110	1.59	30.87
10	11.76	2600	0.015	94	1.61	31.17
11	11.76	2200	0.035	40	1.35	26.19
12	11.76	2600	0.035	25	1.00	19.35
13	11.76	2400	0.025	55	1.45	28.06
14	11.76	2400	0.025	57	1.50	29.08
15	11.76	2400	0.025	56	1.48	28.57

β and average γ of fifteen specimens varied parameters are given in Table 2, which reveals that there are no obvious HAZ and defects on CFRP surface.

As shown in Fig. 3, the influence of hatch distance is significant. When it increases with the same milling speed and laser power, the depth decreases. Because of lacking of heat, there exist
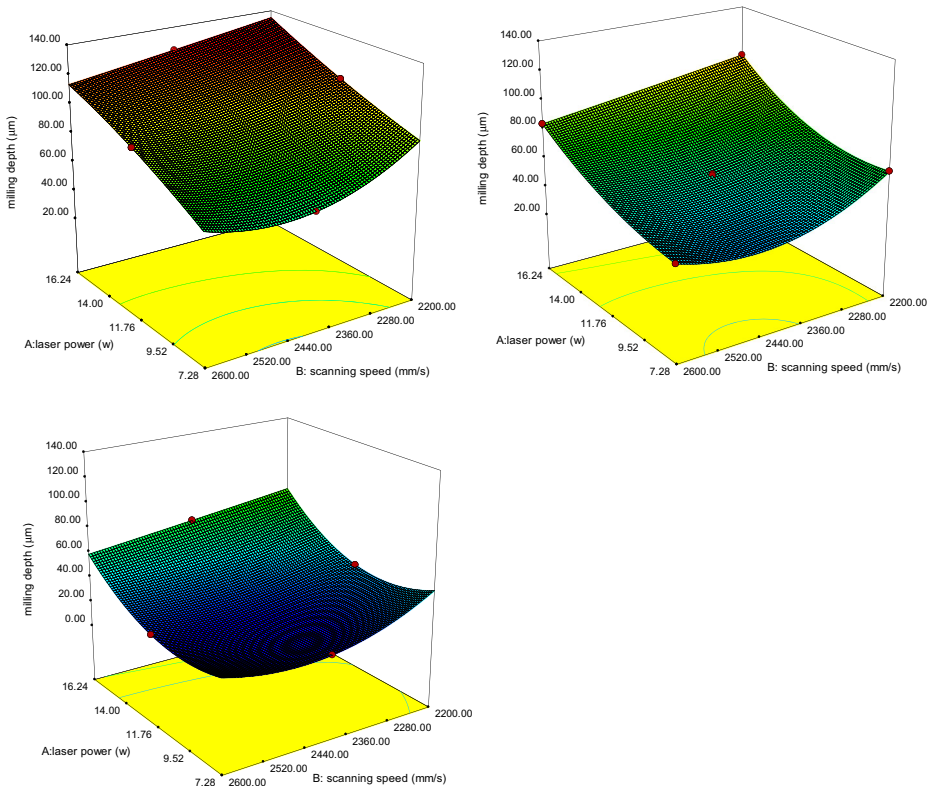

Fig. 3 Effect of laser power and scanning speed on milling depth (d = 0.015, 0.025, 0.035 mm)
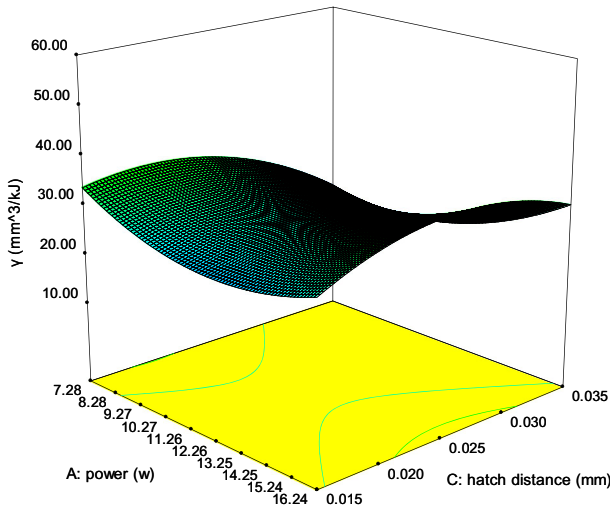
Fig. 4 Effect of laser power and hatch distance on material removal rate (v = 2500 mm/s)

unprocessed material between two tracks with hatch distance increasing. Moreover, with fixed hatch distance, the optimal values of milling speed and laser power can be obtained. In addition, slower milling speed and larger laser power result in deeper milling depth. The deepest specimen was milled at $p = 16.24$ W, $v = 2200$ mm/s and $d = 0.015$ mm, however, it doesn't gain the best surface quality. There are some residual fibers on this milled surface because of resin pyrolysis. The shallowest specimen was milled at $p = 7.28$ W, $v = 2600$ mm/s and $d = 0.035$ mm. The same depth can be milled at the combination of three different parameters, however, the surface quality are different. In order to get optimized parameters, depths and surface quality were taken into account, and when it was milled at $p = 11.76$w, $v = 2200$ mm/s, and $d = 0.015$ mm, there are no defects on the milled surface and the depth is 110 μm.

Figure 4 shows the influence of hatch distance and laser power on material removal rate at $v = 2500$ mm/s. There is an optimal laser power with different hatch distance for the maximal
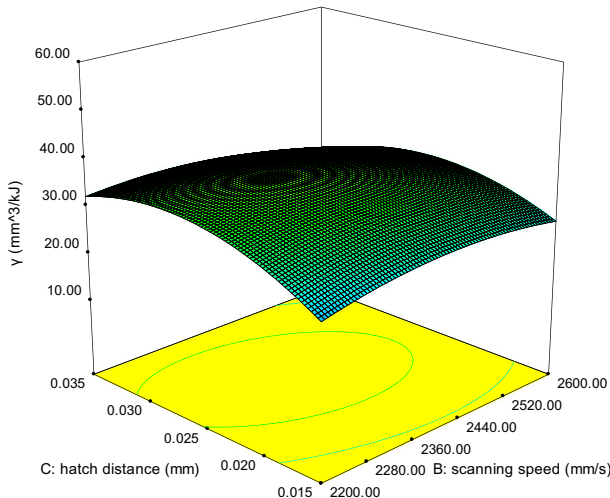

Fig. 5 Effect of hatch distance and hatch distance on material removal rate ($p = 16$ W)
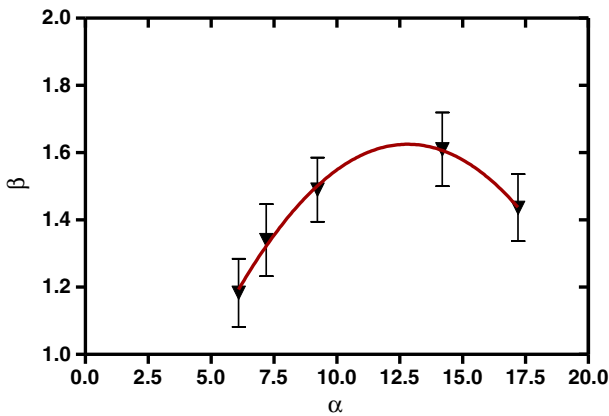
Fig. 6 The relationship between laser beam overlap ratio and β at p = 11.76 W

value of material removal rate. With hatch distance increases, material removal rate increases and then drops because smaller hatch distance results in material removing without mechanical denudation and some carbon fiber can't be ablated at larger hatch distance.

The horizontal distance between pulses is determined by scanning speed. With the decrease of scanning speed, the horizontal distance decreases and material removal rate increases in Fig. 5. In order to get the maximal material removal rate, horizontal distance and hatch distance should be optimized.

The relationship between β and laser beam overlap ratio was studied at p = 11.76 W. As shown in Fig. 6, when laser beam overlap ratio is less than 12.5, β increases along with laser beam overlap ratio because enough recoil pressure was gained to remove the material between adjacent tracks. The maximal β is 1.6 and after that it declines with the increase of laser beam overlap ratio because the material were ablated directly. Compared to our previous research, laser beam overlap ratio is larger than before and β was close to 1. It means that the influence of recoil pressure is not significant with picosecond pulsed laser milling.
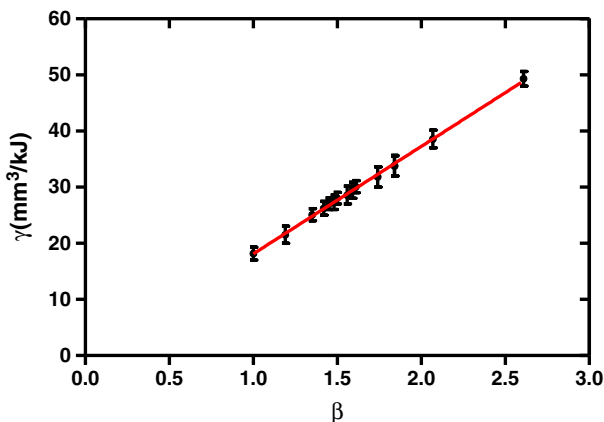

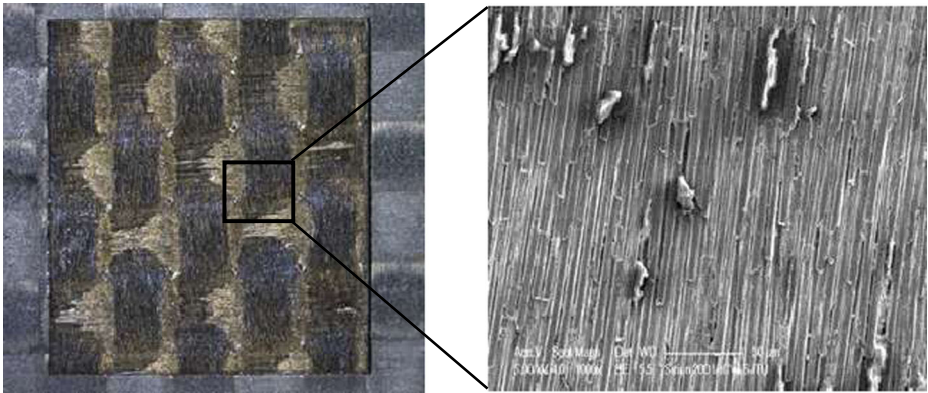**Fig. 7** The relationship between material removal rate and β

Fig. 8 Microstructure of milled surface (p = 14.32w, v = 2200 mm/s, d = 0.01 mm)

Figure 7 gives the relationship between material removal rate and β. With the increase of β, material removal rate increases linearly. Mechanical denudation plays important role in laser milling and γ can be improved through it.

3.2 Microstructure of Specimens

The machined surfaces of three specimens varied parameters were observed with scanning electron microscope. Figure 8 exhibits the microstructure of surface milled at $p = 14.32w$, $v = 2200$ mm/s, and d = 0.01 mm. The twill weave ply was observed obviously because the milling depth is smaller than 0.3 mm. There are many carbon fibers with different length because of uneven energy. Larger HAZ was significant due to 0.01 mm hatch distance which is smaller than the spot size of the laser beam (21 μm). This means there are overlaps of two laser beams in milled surface, which increases the accumulated heat and reduces the material removal rate.

Compared with our previous research using nanosecond-pulsed laser, there is no obvious HAZ on the milled surface processed at $p = 16.24w$, $v = 2400$ mm/s, and d = 0.015 mm. As shown in Fig. 9, original morphology features are still maintained, because the single pulse
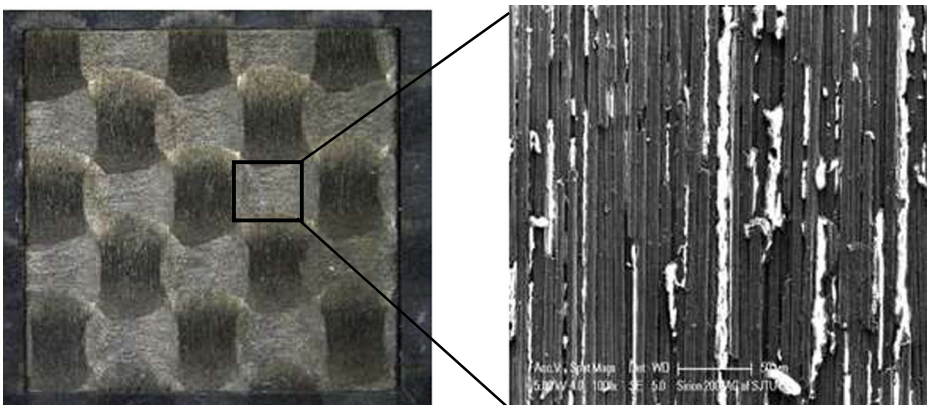

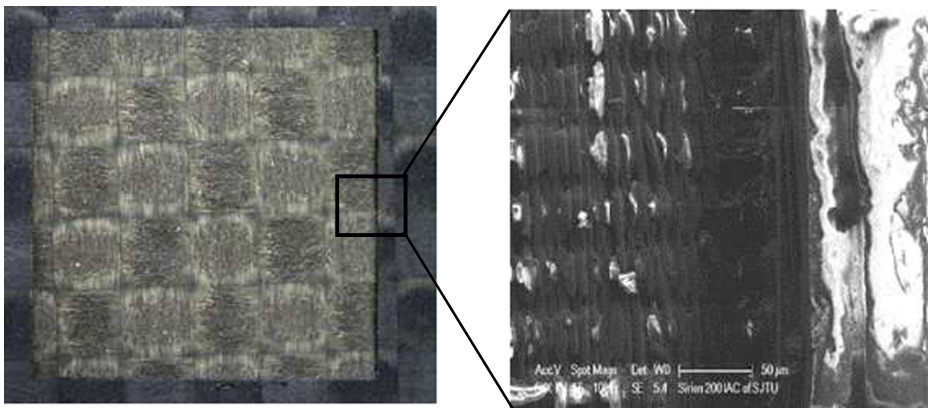**Fig. 9** Microstructure of milled surface (p = 16.24w, v = 2400 mm/s, d = 0.015 mm)

Fig. 10 Microstructure of milled surface (p = 7.28w, v = 2400 mm/s, d = 0.035 mm)

width (10 ps) is so short that the heat can't transfer along the carbon fiber and it can't gain enough heat to result in resin pyrolysis, so picosecond-pulsed laser can compress the HAZ. When it comes to UV laser, the removal mechanism of epoxy resin is different. The energy of photon is higher than the bond energy of resin, so that it can break the bond directly, however, there still exist some resin pyrolysis. It means the resin removal mechanisms are composed of photon thermal effects and photon chemical effects.

As depicted in Fig. 10, fiber chips between the tracks can be seen at p = 7.28w, v = 2400 mm/s, and d = 0.035 mm. The hatch distance is larger than 0.021 mm and the heat can't vaporize the fibers because of low laser power.

When hatch distance was 0.025 mm and still larger than 0.021 mm, no fiber chips were observed in milled regions. As shown in Fig. 11, between the two tracks, the accumulated heat results in resin pyrolysis with various gases and enough vaporization recoil pressure was
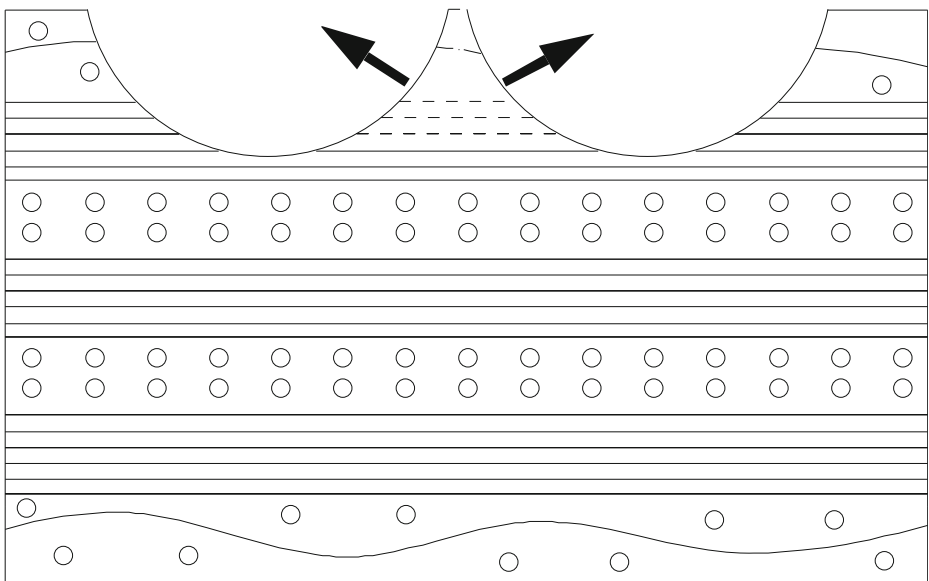

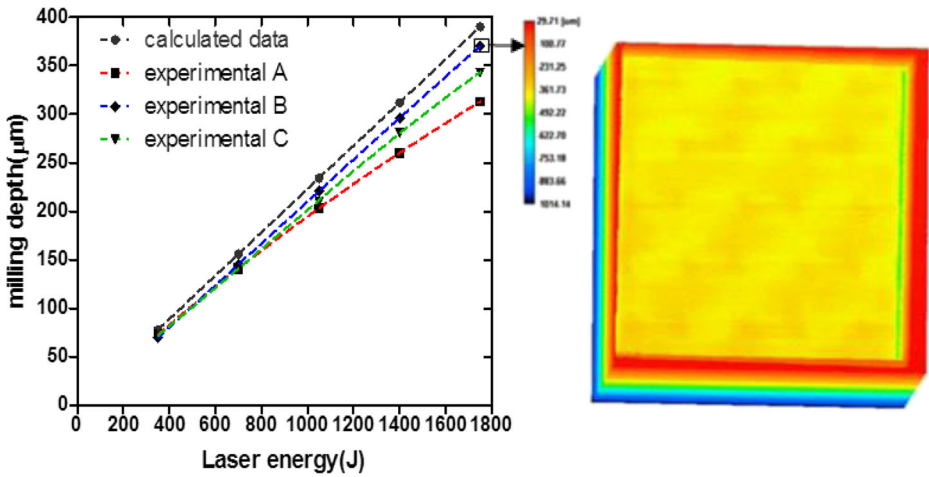**Fig. 11** Removal schematic of two contiguous tracks

Fig. 12 Three groups of experiments with different focal plane

gained to eject fibers. Through this research, the laser milling with optimal parameters can not only avoid fiber chips but also reduce HAZ. This fiber chips removal mechanism suppresses HAZ and increases the material removal rate.

3.3 CFRP re-Focusing Technique

This experiment was processed at $p = 11.76w$, $v = 2200$ mm/s, and $d = 0.015$ mm. There are three groups of experiments: A, B, and C. In each group, five specimens were milled at 10, 20, 30, 40, and 50 scanning passes, respectively. In experiment A, the focal plane is always located on the original specimen surface with fixed z axis. For experiment B and C, z axis moves down by 0.1 mm and 0.2 mm for every 10 scanning passes, respectively. Figure 12 exhibits that the deepest processed specimen is 364 μm measured with the three dimensional profilometer, because the focal plane can follow milled surface in experiment B and it is close to the theoretical value. For experiment A, it can't focus on the milled surface and got the shallowest depth. In addition, the focal plane is lower than milled surface in experiment C. In order to improve the material removal rate, the focal plane is expected to follow milled surface. The depths of each milling with different parameters are not the same. So there is an optimal value of moving down in z axis for different combination of parameters. For this experiment, the optimal value is 0.2 mm. As shown in Fig.
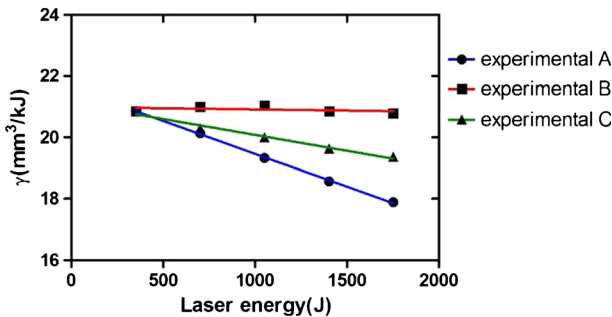

Fig. 13 Variation of γ with increasing milling passes

10, the milling depth is proportional to laser energy in experiment B. It means that there are no accumulated heat which affect the under material.

Figure 13 shows that the material removal rate is constant in experimental A and in other experiments it decreases with the increase of laser energy. In addition, the maximal value of γ was gained in experimental A. In other words, the focal plane can follow the milled surface through z axis moving down by 0.2 mm for every 10 scanning passes which is the optimal value.

4 Conclusion

In order to gain optimum CFRP milling conditions, a Nd:YVO$_4$ picosecond pulsed system emitting at 355 nm was adopted and the influence of milling parameters on surface quality and material removal rate was studied. The three dimensional plots were gained to analyze the influence trends of the parameters. In optimized milling conditions, no significant HAZ could be observed and a re-focusing technique was presented. The conclusions elucidated are as follows:

Laser milling of CFRP is complex and the optimized laser power, milling speed and hatch distance are found to be 11.76w, 2200 mm/s and 0.015 mm respectively. Compared to CFRP machining using nanosecond-pulsed laser, HAZ can be compressed in this laser source at optimized parameters. And laser beam overlap ratio is larger than before which is determined by horizontal distance between pulses and hatch distance. Material removal mechanisms are composed of photon thermal effects, photon chemical effects and mechanical effects, however, mechanical effects is not significant due to the mechanical denudation factor is close to 1 which is different from nanosecond-pulsed laser milling.

Laser beam defocusing results in the decrease of material removal rate in industrial application. Through the experimental investigation, the optimal controlled value at these parameters was gained and it was close to the theoretical value. Material removal rate was studied with increasing milling passes and it was found that this re-focusing technique can improve material removal rate.

References

1. Katnam, K.B., Silva, L.F.M.D., Young, T.M.: Bonded repair of composite aircraft structures: a review of scientific challenges and opportunities. Prog. Aerosp. Sci. **61**, 26–42 (2013)
2. Tagliaferri, V., Ilio, A.D., Visconti, C.: Laser cutting of fibre-reinforced polyesters. Composites. **16**(4), 317–325 (1985)
3. Goeke, A., Emmelmann, C.: Influence of laser cutting parameters on CFRP part quality. Phys Procedia. **5**(Part B), 253–258 (2010)
4. Hu, N.S., Zhang, L.C.: Some observations in grinding unidirectional carbon fibre-reinforced plastics. J. Mater. Process. Technol. **152**(3), 333–338 (2004)
5. Bhatnagar, N., Ramakrishnan, N., Naik, N.K., et al.: On the machining of fiber reinforced plastic (FRP) composite laminates. Int J Mach Tool Manu. **35**(5), 701–716 (1995)
6. Krishnaraj, V., Prabukarthi, A., Ramanathan, A., et al.: Optimization of machining parameters at high speed drilling of carbon fiber reinforced plastic (CFRP) laminates. Compos Part B Eng. **43**(4), 1791–1799 (2012)
7. Srinivasu, D.S., Axinte, D.A.: Mask-less pocket milling of composites by abrasive Waterjets: an experimental investigation. J Manuf Sci Eng. **136**(4), 041005 (2014)

8. Al-Sulaiman, F.A., Yilbas, B.S., Ahsan, M., et al.: Laser hole Drilling of Composites and Steel Workpieces. Lasers Eng. **16**(1), 105–120 (2006)
9. Yung, K.C., Mei, S.M., Yue, T.M.: A study of the heat-affected zone in the UV YAG laser drilling of GFRP materials. J. Mater. Process. Technol. **122**(2–3), 278–285 (2002)
10. Davim, J.P., Barricas, N., Conceição, M., et al.: Some experimental studies on CO 2, laser cutting quality of polymeric materials. J. Mater. Process. Technol. **198**(1–3), 99–104 (2008)
11. Wolynski, A., Herrmann, T., Mucha, P., et al.: Laser ablation of CFRP using picosecond laser pulses at different wavelengths from UV to IR. Phys. Procedia. **12**(1), 292–301 (2011)
12. Sugioka, K., Cheng, Y.: REVIEW ultrafast lasers—reliable tools for advanced materials processing. Light Sci Appl. **3**(4), e149 (2014)
13. Hu, J., Xu, H.: Pocket milling of carbon fiber-reinforced plastics using 532-nm nanosecond pulsed laser: An experimental investigation. J. Compos. Mater. **50**(20), (2015)